

Comparative Bio-sorption of Cadmium and Nickel Ions from Aqueous Solution onto Fibers of Date Palm using Fluidized Bed Column

BAKER M. ABOD¹, RAMY MOHAMED JEBIR AL-ALAWY¹, FIRAS HASHIM KAMAR¹, GHEORGHE NECHIFOR^{2*}

¹ Institute of Technology- Baghdad, Middle Technical University, Iraq

² University Politehnica of Bucharest, Department of Analytical Chemistry and Environmental Engineering, 1-7 Gheorghe Polizu Str., 011061, Bucharest, Romania

The aim of this study is to use the dry fibers of date palm as low-cost biosorbent for the removal of Cd(II), and Ni(II) ions from aqueous solution by fluidized bed column. The effects of many operating conditions such as superficial velocity, static bed height, and initial concentration on the removal efficiency of metal ions were investigated. FTIR analyses clarified that hydroxyl, amine and carboxyl groups could be very effective for bio-sorption of these heavy metal ions. SEM images showed that dry fibers of date palm have a high porosity and that metal ions can be trapped and sorbed into pores. The results show that a bed height of 6 cm, velocity of 1.1U_{mf} and initial concentration for each heavy metal ions of 50 mg/L are most feasible and give high removal efficiency. The fluidized bed reactor was modeled using ideal plug flow and this model was solved numerically by utilizing the MATLAB software for fitting the measured breakthrough results. The breakthrough curves for metal ions gave the order of bio-sorption capacity as follow: Cd(II) > Ni(II).

Keywords: Bio-sorption, fluidized bed reactor, fibers of date palm, heavy metals ions

The using of new techniques led to the development rapidly of production in industrial and agricultural fields which has occurred in recent years has led to increasing water and soil pollution in heavy metal ions and dyes [1, 2].

The metals can be classified depending on the risky to three groups: the first representing toxic metals (Hg, Cr, Pb, Zn, Cu, Ni, Cd, As, Co, Sn, etc.), and second group containing precious metals (Pt, Ag, Au, Ru, etc.) while the third containing radionuclides (U, Th, Ra, Am, etc.) [3].

Cadmium contributes to the spread of some types of cancers in humans, and exposure to low concentrations that lead to damage to the kidney. The poisoning of Cadmium shows two main effects; renal dysfunction and it is often by the oral route [4]. On the other hand, Nickel compounds are considered dangerous environmental pollutants because it is carcinogenic, skin allergy and asthma [5]. The industries of petroleum, refining, metal industries, battery manufacturing processes, catalysts, tanning, photographic, ceramic and glass industries, electroplating and etc. represents the main source of pollution because the producing great quantities of effluent water containing heavy metals [6].

Generally, the major problem of contamination of heavy metal for the environment is caused by its toxicity and accumulation in the human bodies through it entering the food chain. Therefore, disposal of the heavy metals in wastewater is important to the environmental protection and the healthiness of human [7].

There are several methods to remove heavy metals, from the effluent of industrial water such as sedimentation, flotation, lime coagulation, ion exchange, electrical dialysis, reverse osmosis, membrane, adsorption, etc. but not all these techniques are eco-friendly, and each of these has advantages and disadvantages, that depends on the costs of the operation or/and maintenance [8, 9]. But the

adsorption method is one of the efficient and economic methods in terms of the cost of manufacturing, operation, and maintenance if compared to other methods [10].

In the recent years, bio-sorption technology was used because of the major advantages: high effectiveness to reduce the heavy metal ions concentration to very low levels, an environment-friendly and economically [11]. Algae, fungi, bacteria, and yeasts have proved to be potential metal biosorbents [12].

There are many recent studies, focused to develop cheap and effective adsorbents from the abundant sources of naturalistic agriculture wastes and using to remove the heavy metal ions from aqueous solution. The agriculture wastes represent efficient low-cost adsorbents material are used to removal of heavy metals such as rice husk, walnut shells, sawdust, green coconut shells, apple waste, waste tea leaves, cabbage leaves, peanut and hazelnut shells [13-15].

Recently, the agriculture wastes were widely used to bio-sorption of heavy metal ions in fluidized bed reactors. These systems are achieved a good contact between the particles of the bed and the available fluid which can be ensured the required mass transfer [16].

The main aims of this study are: (i) characterization the physical and chemical properties of dry fibers of date palm (FDP) used as bio-sorbent (ii) estimation the breakthrough curves of Cd(II), and Ni(II) ions using fluidized bed of (FDP) biomass; (iii) evaluation the influence of initial metal concentration, bed depth and superficial velocity on the removal of Cd(II), and Ni(II).

Theoretical Models of Fluidized Bed

The ideal plug flow of the fluid, the uniform distribution of contaminant in the radial direction and no generated byproduct in the reactor are represented the main assumption required for modeling the fluidized bed [17]. Accordingly, the following equations can be written:

$$\left(\begin{array}{c} \text{Rate of input conc. by} \\ \text{convective flow} \end{array} \right) + \left(\begin{array}{c} \text{Rate of input conc. by} \\ \text{dispersion} \end{array} \right) - \left(\begin{array}{c} \text{Rate of output conc. by} \\ \text{convective flow} \end{array} \right) - \left(\begin{array}{c} \text{Rate of output conc. by} \\ \text{dispersion} \end{array} \right) - \left(\begin{array}{c} \text{Solute lost by} \\ \text{sorption} \end{array} \right) = \frac{\partial C}{\partial t} \cdot \varepsilon \cdot dz \quad (1)$$

* email: doru.nechifor@yahoo.com

$$\frac{U}{\varepsilon} \cdot C + E_z \cdot \frac{\partial C}{\partial z} - \frac{U}{\varepsilon} \left[C + \frac{\partial C}{\partial z} dz \right] - E_z \cdot \left[\frac{\partial C}{\partial z} - \frac{\partial}{\partial z} \left(\frac{\partial C}{\partial z} \right) dz \right] - \frac{(1-\varepsilon)}{\varepsilon} \rho_p \frac{\partial q}{\partial t} dz = \frac{\partial C}{\partial t} \cdot dz \quad (2)$$

Then, equation (2) can be written as follows:

$$\frac{U}{\varepsilon} \cdot C + E_z \cdot \frac{\partial C}{\partial z} - \frac{U}{\varepsilon} \cdot C - \frac{U}{\varepsilon} \cdot \frac{\partial C}{\partial z} dz - E_z \cdot \frac{\partial C}{\partial z} + E_z \cdot \frac{\partial^2 C}{\partial z^2} dz - \frac{(1-\varepsilon)}{\varepsilon} \rho_p \frac{\partial q}{\partial t} dz = \frac{\partial C}{\partial t} \cdot dz \quad (3)$$

where ε is the void ratio in the bed, U is the superficial velocity (m/s), C is the metal concentration (mg/L) at time of t and bed height of z , q is the sorbed quantity of the pollutant (mg/g), E_z is the dispersion coefficient in the axial direction (m^2/s).

By simplifying, the following equation can be obtained:

$$\frac{\partial C}{\partial t} = E_z \frac{\partial^2 C}{\partial z^2} - \frac{U}{\varepsilon} \frac{\partial C}{\partial z} - \frac{1-\varepsilon}{\varepsilon} \rho_p \frac{\partial q}{\partial t} \quad (4)$$

Eq. (5) is illustrated the mass conservation of the contaminant on the solid particle:

$$(1 - \varepsilon) \rho_p \frac{\partial q}{\partial t} = K_L \cdot a \cdot (C - C^*) \quad (5)$$

where K_L is the mass transfer constant, C^* is the concentration of metal ion at the equilibrium state (mg/L) and the specific surface area (m^2/m^3) can be designated by a . Combination of eqs. (4) and (5) results the following equation:

$$\frac{\partial C}{\partial t} = E_z \frac{\partial^2 C}{\partial z^2} - \frac{U}{\varepsilon} \frac{\partial C}{\partial z} - \frac{K_L \cdot a}{\varepsilon} (C - C^*) \quad (6)$$

This problem can be subjected to a set of initial and boundary conditions as follows:

$$0 < z < L, \quad t = 0; \quad C = C^* = 0 \quad (7)$$

$$z = 0, \quad t \geq 0; \quad C = C_i \quad (8)$$

$$z = L, \quad t > 0; \quad \frac{\partial C}{\partial z} = 0 \quad (9)$$

where C_i is the initial concentration of the contaminant (mg/L) and H is height of the bed (m),

Eqs. (6)-(9) can be solved by MATLAB software Version (7.9) using numerical method. The theoretical predictions were fitted with experimental measurements for breakthrough curves of the adopted contaminants and coefficient of determination (R^2) was utilized for evaluating the concurrence between predicted and measured results.

Experimental part

Materials and methods

Biosorbent material

The fibers of date palm (FDP) were collected from the local grove and washed twice in distilled water to remove the dust and impurities. It is dried at 65 °C for 2 days using electrical oven, grinded, sieved to 1 mm and it can be used at any time.

Chemicals

A stock solution for each metal (Ni(II) and Cd(II)) was prepared with concentration of 1000 mg/L through dissolved a certain amount of $NiSO_4 \cdot 6H_2O$ and $Cd(NO_3)_2 \cdot 4H_2O$ in distilled water. Lower concentrations were then prepared when required by further dilution of the stock solution with distilled water. The diluted solutions were kept at room temperature. Before the sorption process was initiated, the pH of solutions was adjusted to the required value by adding 0.1 M HCl and 0.1 M NaOH solutions.

Bio-sorption experiments

Glass fluidized bed column was used to procedure bio-sorption experiments (7.5 cm inner diameter and 100 cm high). Stainless steel distributor of 2 mm thickness was installed at the bottom of the reactor to distribute an influent flow smoothly. The U-tube manometer (inside diameter of 5 mm and length of 50 cm) was connected with the column to read the pressure of water in it.

The effects of bed height, the flow rate in a fluidized bed column and the initial concentration of metal ions were studied by carried out a series of single metal solutions experiments for bio-sorption to obtain equilibrium data and breakthrough curves. The optimal operating conditions of pH was 6.5 and 5 for Ni(II) and Cd(II) ions respectively, while the particles diameter was 0.5 mm from the batch experiments according to (Boudaoud, et al., 2017) [18], were adopted in the column experiments. Table 1 show the major parameters used in these experiments.

Results and discussions

Characterization of FDP

The information on nature of interactions between the metal ions and functional groups that found in adsorbent materials by using Fourier transform infrared spectrum (FTIR). Spectrophotometer, (Model: SHIMADZO, 800 series spectra- photometer) in the spectral range of 1000-3500 cm^{-1} was used to investigate the frequency of the functional groups in the dry (FDP).

Figure 1, shows that various functional groups present in the FDP which it's possible that bind with the metal ions. From this figure, the strong band at 3396.64 cm^{-1} indicates the presence of hydroxyl (-OH) and amine (-NH) groups and the peak at 2924.09 cm^{-1} indicates the (C-H) stretching vibration of CH_2 . While the peak at 1625.99 cm^{-1} shows the stretching vibration of carboxyl group (-C=O).

Table 1
MAJOR EXPERIMENTAL PARAMETERS THAT ADOPTED IN FLUIDIZED BED COLUMN

Parameter	Range	Purpose
Bed height	(4, 6 and 8 cm)	To plot the breakthrough curves at different bed height.
Fluid flow rate	Corresponded to 1.1 U_{mf} and 1.5 U_{mf}	To study the variation of breakthrough curves at different flow rate.
Initial concentration of heavy metal ions	50 and 75 mg/L	To plot the breakthrough curves at different Initial concentration.

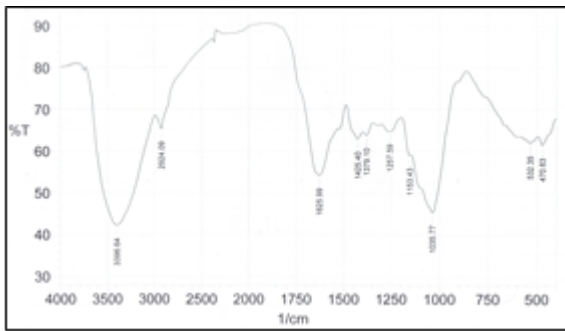


Fig. 1. FTIR spectrum of FDP

Physical properties of the particles of FDP and bed were measured and listed in table 2, because it is very important for application of the fluidized bed models. A scanning electron microscopy (SEM) images for the surface morphology of dry FDP were observed by using an INSPECT-S50, (FEI Co., Netherlands). The SEM images in figure 2; shows that dry FDP particles have numbers of pores and irregular of its surface structure.

Table 2
PARTICLES AND BED PROPERTIES OF FDP USED IN FLUIDIZED BED EXPERIMENTS

Properties	Value
Particle diameter (mm)	0.5
Bulk density (kg/m ³)	410
Real density (kg/m ³)	1025
Surface area (m ² /g)	1.83
Particle porosity (-)	0.402
Bed voidage (-)	0.435

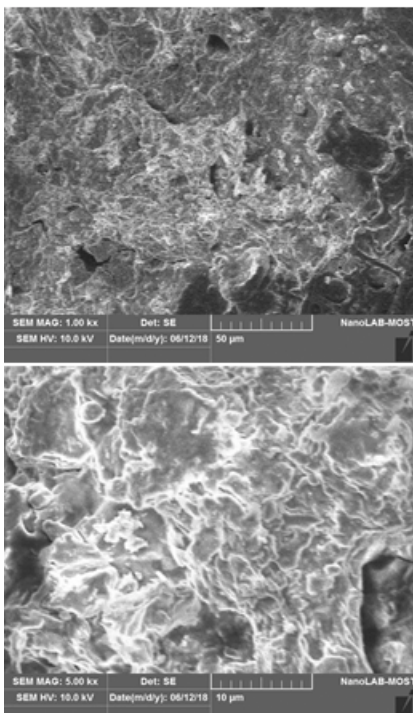


Fig. 2. SEM image of FDP

Fluidized Velocity

The minimum value of fluidization velocity (U_{mf}) is an important parameter in the modeling of fluidized bed reactors because it is one of the fundamental parameters. On the other hand, it is one of the hydrodynamic parameters in the performance and design of fluidized bed reactor [19]. This velocity was specified based on the measurement of the pressure drop through the FDP bed. This process was carried out by partially filling the column with certain

quantity of biomass and then the solid particles were dispersed through the water by agitation. The bed particles were allowed to settle and the discharge was changed progressively from 0 to 100 L/hr. The manometer was used to record the pressure drop for each increment of flow rate.

The experimental values of the U_{mf} were determined by the plot on a logarithmic scale for the pressure drop across the bed versus the superficial liquid velocity. Figure 3, shows that the cross point of the two lines is corresponding to fluidized bed regime and this point represents the U_{mf} . It is clear that the drop in the pressure was varied linearly below the U_{mf} . In addition, the finding the relationship between the voids of the bed and superficial velocity is important in the modeling of a fluidized bed [20]. The ϵ is represented by the difference between the total volume of the fluidized bed and the volume of the particles as follows:

$$\epsilon = \frac{V_\epsilon}{V_b} = \frac{V_b - V_p}{V_b} = 1 - \frac{V_p}{V_b} = 1 - \frac{m_p}{\rho_p V_b} = 1 - \frac{m_p}{\rho_p A H} \quad (9)$$

where m_p is the used mass (kg), A is the area of the reactor (m²), ρ_p is the particle density (kg/m³), H is the expanded height of the bed (m).

Table 3 elucidates the (U_{mf}), plateau pressure drop ΔP and expanded of bed height (h_{mf}) at a cross section area of the bed is 0.0441 m².

In this study, the biosorption experiments were carried out using fluidizing velocities correspondent to 1.1 and 1.5 U_{mf} in order to preserve the fluidization phenomena until the end of continuous process experiments.

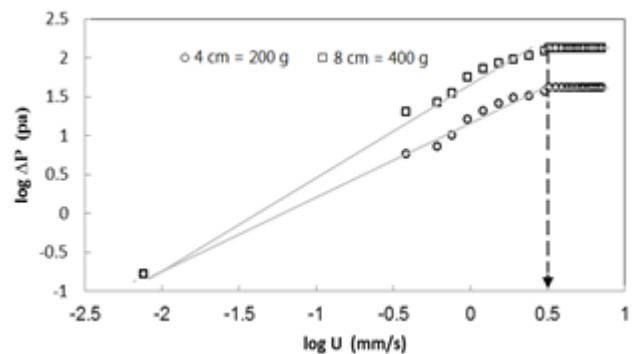


Fig. 3. Pressure drop vs. superficial fluid velocity of two weights of dry FDP

Table 3

U_{mf} , ΔP AND h_{mf} of 0.5 mm SIZE FDP BED PARTICLES			
Static height (cm)	U_{mf} (mm/s)	ΔP (pa)	h_{mf} (cm)
1	3.000	40.139	2.8
2		81.673	5.7
4		132.962	10.5
6		190.56	14.3
8		227.45	22.4
10		265.78	30.1

Bed expansion

The relationship between the superficial liquid velocity (U) and the bed voidage (ϵ) is very important and it can be established using equations (10) [21]. Figure 4 shows the variation of bed voidage of FDP with the liquid velocity. The relationship obtained from this figure will be very useful in the modeling of fluidized bed reactor.

$$U/U_i = \epsilon^n \quad (10)$$

where U is the superficial velocity that corresponded to U_{mf} and U_i is the settling velocity for a particle of dry FDP at infinite dilution. The index (n) is constant represent a

function of Reynolds number (Re_t) and particle terminal velocity.

Richardson and Zaki using the following relationships to calculate U_i and n as follows:

$$n = (4.4 + 18 d/D) Re_t^{-0.1} \quad (1 < Re_t < 200) \quad (11)$$

where d is the diameter of FDP particle; D is the fluidized bed diameter.

The values of (U) and the terminal velocity (U_t) are related by:

$$\log U_i = \log U_t - \frac{d}{D} \quad (12)$$

where U_t is the terminal free-falling velocity; Re_t is the Reynolds number at terminal velocity.

$$Re_t = \frac{U_t \cdot d \cdot \rho_f}{\mu_f}$$

$$U_t = \frac{0.153 \cdot g^{0.71} \cdot d_p^{1.14} \cdot (\rho_s - \rho_f)^{0.71}}{\rho_f^{0.29} \cdot \mu_f^{0.48}} \quad (Re_p > 0.2) \quad (14)$$

In addition, eq. (9) using to find the experimental value of (ε) for fluidized dry FDP and it is found to be equal 0.5. But this value is lower than the calculated value (0.525). The Richardson-Zaki equation is based on the fact that particles are a homogeneous and spherical shape in the fluidized bed; therefore, this may be possible [22].

Where ρ_s is the density of the particle in the fluid; ρ_f is the density of the fluid; μ_f is the viscosity of the fluid, and Re_t is the particle Reynolds number.

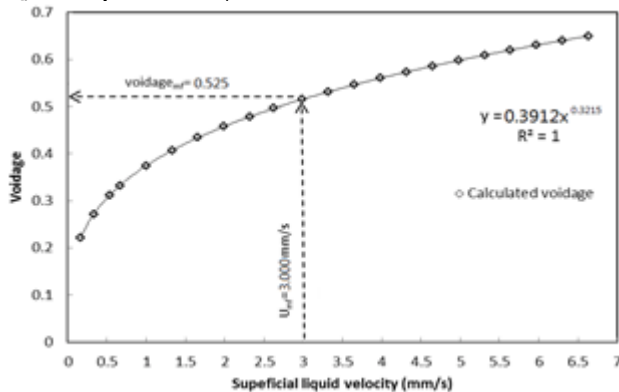


Fig. 4. Variation of dry FDP bed voidage with the superficial liquid velocity

Mass transfer coefficient

The mass transfer coefficient is one of the important parameters in the modeling of fluidized bed reactor. Further, knowledge of the values of mass transfer coefficients for all of the ionic species in the fluidized bed system is required. In the literature, there are numerous correlations to estimate the mass transfer coefficient (K_L) of a fluidized bed and most of them are valid for continuous systems. The correlation presented by [17] was adopted in the present study after developed according to a fluidized bed conditions to the following equation:

$$\frac{Sh \cdot \varepsilon^{1/3}}{Sc^{1/3}} = 0.62 Re_p + 0.6 \quad (15)$$

Metal	$D_m \cdot 10^{10}$ m ² /s	Sc	$1.1 U_{mf}$				$1.5 U_{mf}$			
			Re_p	ε	Sh	$K_L \cdot 10^4$ (m/s)	Re_p	ε	Sh	$K_L \cdot 10^4$ (m/s)
Cd(II)	5.425	1854.37	3.134	0.496	39.366	0.206	4.268	0.536	48.687	0.233
Ni(II)	6.453	1624.69			36.542	0.285			46.146	0.287

Table 4
CALCULATED K_L VALUES
OF Cd(II), and Ni(II) AT
TWO FLOW RATE

where Sh is the Sherwood number ($K_L \cdot d / D_m$), Sc is the Schmidt number (ν / D_m), and D_m is the liquid phase diffusivity (m²/s). The relation between liquid kinematic viscosity: ν (m²/s), and the liquid phase diffusivity: D_m (m²/s), using to calculated Schmidt number by this equation: ($Sc = \nu / D_m$). Liquid phase diffusivity calculated according to equation below [23]:

$$D_m = 2.74 \cdot 10^{-9} (M_w)^{-1/3} \quad (16)$$

The results of D_m , Sc , and K_L for each metal at U_{mf} and 0.5 mm diameter of FDP particles are listed in table 4.

Breakthrough curves

The breakthrough curves parameters for the single system for two heavy metals were obtained by carried out a series of single continuous experiments after measuring the (ΔP , U_{mf} and ε). The continuous experiments were carried out at bed heights (4, 6, and 8 cm), flow rates (43 and 61) L/h, corresponded to ($1.1 U_{mf}$ and $1.5 U_{mf}$), and particle diameters (0.5 mm).

These curves are plotted the relation between C/C_0 and time for each metal. Breakthrough curves generally permit a good description of the processes in bio-sorption columns. The experimental and predicted breakthrough curves are presented at different operating conditions depending on various hydrodynamic parameters such as bed weight, flow rate and initial metal concentrations of heavy metal. Also, the equilibrium bio-sorption isotherm and mass transfer rate are represented main important factors on the shape and sharpness of the breakthrough curve [24].

Effect of Bed height

The effect of bed height of dry FDP on the biosorption process at $U = 1.1 U_{mf}$, $C_0 = 50$ ppm, $d_p = 0.5$ mm and corresponding to static bed heights 4, 6 and 8 cm was investigated and presented in figures (5 and 6). It can be seen from these figures that a major affect for the bed heights on bio-sorption of metal ions in the column. This helps us to predict the volumes of treated bed for large-scale applications.

In these figures, it was found that the breakpoint time for Ni(II) ions appears earlier than that for Cd(II). In other words, the adsorption rate of Cd(II) ions is greater than Ni(II) ions due to highest breakpoint time. These results are in a good agreement with [25].

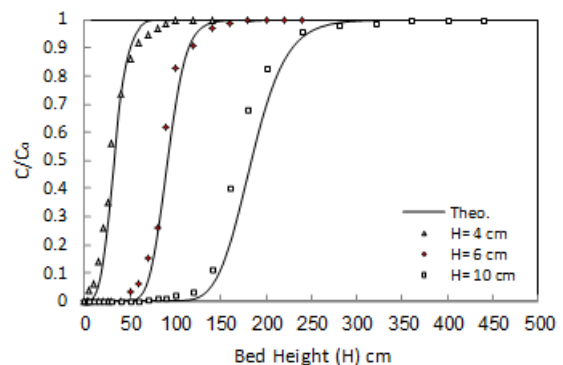


Fig. 5. Experimental data and theoretical breakthrough curves for bio-sorption of Cd(II) at different bed height, $C_0 = 50$ mg/L, $U = 1.1 U_{mf}$, $d_p = 0.5$ mm

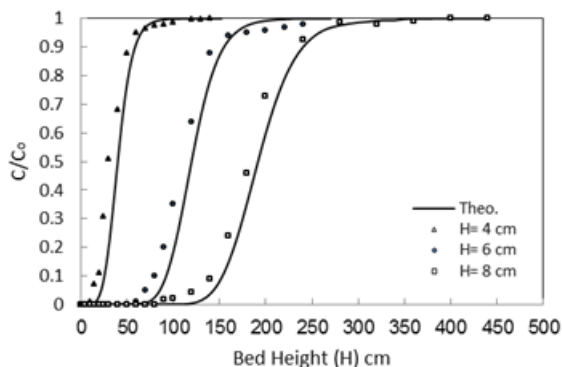


Fig. 6. Experimental data and theoretical breakthrough curves for bio-sorption of Ni(II) at different bed weight, $C_o=50$ mg/L, $U=1.1U_{mf}$, $d_p=0.5$ mm

Although an increasing bed height of 6 cm increased the bed volume and contact time for each metal, it appeared that two metals reach the breakthrough at the same time. This means that the increasing of contact time between contaminant and FDP for higher bed height. Also, an increase in the bed height will increase the surface area or bio-sorption sites which improve the bio-sorption process.

Effect of Flow Rate

The design of fluidized bed reactor is depended on the value of fluid flow rate because it is specified the required time for contact between the sorbate and sorbent. It was found that the increase of fluid flow rate leads to a decrease in the surface area of the adsorbent material per volume of a column, and increase the voidage of the fluidized bed increased [26].

The breakthrough curves that obtained for different fluid flow rate correspondent to $U=1.1U_{mf}$ and $U=1.5U_{mf}$, shown in figures (7 and 8). All these experiments were carried out at the same static bed height (6 cm) and initial concentrations (50 mg/L) for two pollutant materials. These figures show the breakthrough curves become steeper when the flow rate increases for two heavy metal ions.

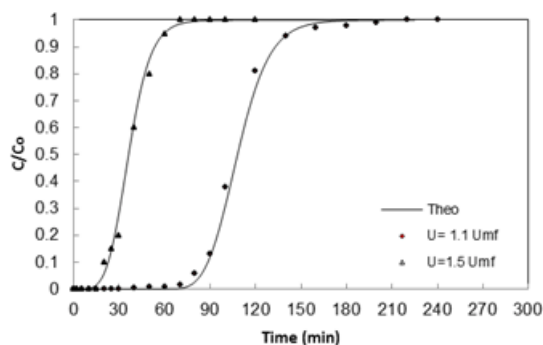


Fig. 7. Experimental data and theoretical breakthrough curves for bio-sorption of Cd(II) at different fluid velocity, $C_o=50$ mg/L, 6 cm bed height, $d_p=0.5$ mm.

Figures (7 and 8) show also, the biosorption capacity of the fluidized bed column had a better performance at lower flow rates. Because, at a higher flow rate it was lower due to insufficient residence time between metals ions and a bed in the column, and therefore, the solute left the column before equilibrium occurred. Therefore, increasing the flow rate will decrease the volume treated until reaching the breakthrough point, therefore, that decreases the operational time of the bed [27].

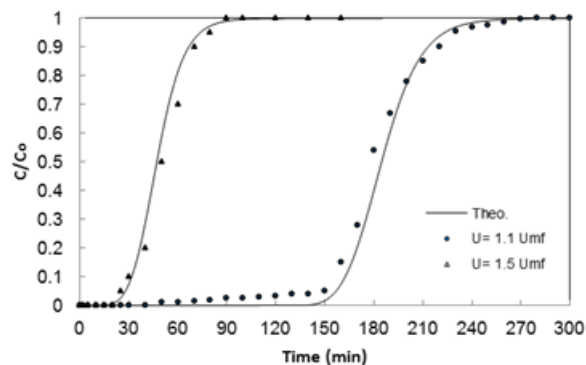


Fig. 8. Experimental data and theoretical breakthrough curves for bio-sorption of Ni(II) at different fluid velocity, $C_o=50$ mg/L, 6 cm bed height, $d_p=0.5$ mm

Effect of Initial Metals Concentration

The breakthrough curves of the dry FDP onto Cd(II) and Ni(II) metals at fixed bed height of 6 cm, fluid velocity ($U=1.1U_{mf}$) and different initial concentrations (50 and 75 mg/L), are shown in figures (9 and 10). These two figures indicated that the breakthrough point of Cd(II) and Ni(II) ions was decreased with an increase in the initial concentrations from 50 to 75 mg/L for two heavy metal ions. This is due to, the saturation of the available binding sites on the surface area that present in the fluidized bed in the range of initial concentration of metal ions from 50 to 75 mg/L, similar to that observed by [21].

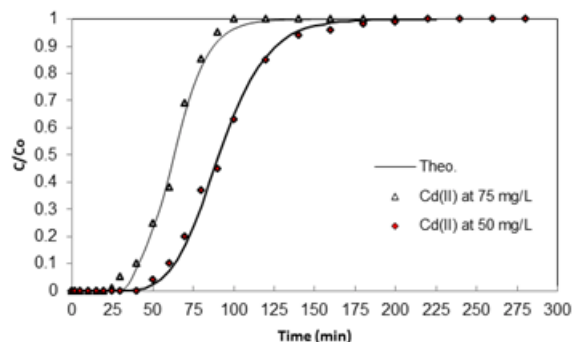


Fig. 9. Experimental data and theoretical breakthrough curves for bio-sorption of Cd(II) at different initial metal concentration, $U=1.1U_{mf}$, 6 cm bed height, $d_p=0.5$ mm.

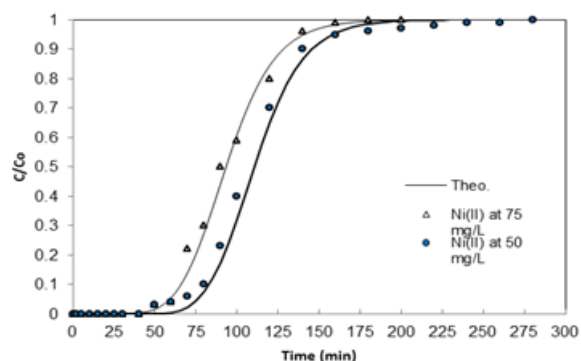


Fig. 10. Experimental data and theoretical breakthrough curves for bio-sorption of Ni(II) at different initial metal concentration, $U=1.1U_{mf}$, 6 cm bed height, $d_p=0.5$ mm

Conclusions

A fluidized bed reactor can be applied for the continuous removal of Cd(II) and Ni(II) ions using particles of dry fibers of date palm (FDP) bed. The minimum fluidization velocity was found equal to 3.00 mm/s at 0.5 mm particles size. The experimental breakthrough data of two metal ions are

fitted well with the theoretical model. The Cd(II) ions showed the largest breakthrough time compared with Ni(II) ions. In the fluidized system, the greater height of the FDP bed can be increased effectively the breakthrough time. While the increasing contaminated water discharge can be caused a decrease in the breakthrough time. Conversely, the low values of discharge are resulted in the increasing of contact time to occupy all the spaces within the particles. In addition, the breakthrough time is decreasing with increasing of initial concentration for heavy metal ions. The biosorption capacity arranges for the single systems are Cd(II) > Ni(II).

References

1. NOCITO, F., LANCILLI, C., GIACOMINI, B. and SACCHI, G. A., Sulfur Metabolism and Cadmium Stress in Higher Plants, *Plant Stress*, Global Science Books, **1**, No. 2, 2007, p. 142.
2. TZU, T. W., TSURITANI, T., SATO, K., Sorption of Pb(II), Cd(II), and Ni(II) toxic metal ions by alginate-bentonite, *J. Environ.*, **4**, 2013, p. 51.
- 3*** World Health Organization, Guidelines for drinking Water Quality, Geneva, 1984.
- 4 NOSIER, S. A., Removal of Cadmium Ions from Industrial Wastewater by Cementation. *Chem. Biochem. Eng. Q.*, **17**, No. 3, 2003, p. 219.
5. ASLAM, M. Z., RAMZAN, N., NAVEED, S., and FEROUZE, N., Ni (II) Removal by biosorption using ficus religiosa (peepal) leaves, *J. Chil. Chem. Soc.*, **55**, No. 1, 2010, p. 81.
6. ARSALANI, N., RAKH, R., GHASEMI, E., and ENTEZAMI, A., Removal of Ni(II) From Synthetic Solutions Using New Amine-containing Resins Based on Polyacrylonitrile, *Iranian Polymer Journal*, **18**, No. 8, 2009, p. 623.
7. VIMALA, R. and NILANJANA, DAS, Biosorption of cadmium (II) and lead (II) from aqueous solutions using mushrooms: A comparative study, *J. Hazardous Materials*, **168**, No. 1, 2009, p. 376..
8. CAROLINE, B., MEURIS, G., ERIC, G., Chromium biosorption using the residue of alginate extraction from sargassum filipendula, *Chem. Eng. J.*, **237**, 2014, p. 362.
9. TADJARODI, A., JALALAT, V., ZARE-DORABEL, R., Adsorption of La(III) in aqueous systems by N-(2-hydroxyethyl) salicylaldimine-functionalized mesoporous silica, *Mat. Res. Bull.*, **61**, 2015, p. 113.
10. ALLEY, E. R., *Water quality control handbook*, 2nd Ed., McGraw-Hill Companies, Inc., USA, **2006**.
11. GUPTA, V. K., RASTOGI, A., Equilibrium and kinetic modelling of cadmium(II) biosorption by nonliving algal biomass *Oedogonium* sp. from aqueous phase, *J. Hazard. Mater.*, **153**, 2008, p. 759.
12. KAMAR, F. H., NECHIFOR, A. C., NECHIFOR, G. AL-MUSAWI, T. J., MOHAMMED, A. H., Aqueous Phase Biosorption of Pb(II), Cu(II), and Cd(II) onto Cabbage Leaves Powder, *Int. J. Chem. React. Eng.*, **15**, No. 2, 2016, p. 1.
13. RATHINAM, A., MAHARSHI, B., JANARDHANAN, SK., JONNALAGADDA, R., NAIR, BU., Biosorption of cadmium metal ion from simulated wastewater using *Hypnea valentiae* biomass: a kinetic and thermodynamic study, *J. Bioresour. Tech.*, **101**, No. 5, 2009, p. 1466.
14. KAMAR, F. H., NECHIFOR, A. C., NECHIFOR, G., SALLOMI, M. H., JASEM, A. D., Study of the Single and Binary Batch Systems to Remove Copper and Cadmium Ions from Aqueous Solutions using Dry Cabbage Leaves as Biosorbent Material, *Rev. Chim. (Bucharest)*, **67**, no. 1, 2016, p. 1.
15. KAMAR, F. H., ABBAS, S. H., MOHAMMED, A. H., CRACIUN, M. E., NECHIFOR, A. C., Isotherm and Kinetic Models for Bio-sorption of Cadmium Ions from Aqueous Solutions using Dry Peanut Shells and Hazelnut Shells, *Rev. Chim. (Bucharest)*, **69**, no. 10, 2018, p. 2603.
16. PARK, Y. G., CHO, S. Y., KIM, S. J., LEE, G. B., KIM, B. H., PARK, S. J., Mass transfer in semi-fluidized and fluidized ion-exchange beds, *Environ. Eng. Res.*, **4**, No. 2, 1999, p. 71.
17. KOSTOV, G., ANGELOV, M., MIHAILOV, I. and STOIEVA, D., Development of combined models to describe the residence time distribution in fluidized-bed bioreactor with light beads, *Procedia Food Science*, **1**, 2011, p. 770.
18. BOUDAOU, A., DJEDID, M., BENALIA, M., Ad, C., BOUZAR, N., ELMSELLEM, H., Removal OF Nickel (II) and Cadmium (II) Ions from Wastewater by Palm Fibers, *Scientific Study & Research Chemistry & Chemical Engineering, Biotechnology, Food Industry*, **18**, No. 4, 2017, p. 391.
19. NIDAL, H., GHANNAM, M., ANABTAWI, M., Effect of bed diameter, Distributor and Inserts on minimum fluidization velocity, *Chem. Eng. Technol.*, **24**, No. 2, 2001, p. 161.
20. SULAYMON, A. H., MOHAMMED, A. A., AL-MUSAWI, T. J., Column Biosorption of Lead, Cadmium, Copper, and Arsenic ions onto Algae. *J Bioprocess Biotech* 3: 128 doi: 10.4172/2155-9821.1000128, (2013).
21. KAMAR, F. H., MOHAMMED, A. A., FAISAL, A. A. H., NECHIFOR, A. C., NECHIFOR, G., Biosorption of Lead, Copper and Cadmium Ions from Industrial Wastewater Using Fluidized Bed of Dry Cabbage Leaves, *Rev. Chim.(Bucharest)*, **67**, no. 6, 2016, p. 1039.
22. MAZUMDER, J., ZHU, J., RAY, A., Optimal design of liquid-solid circulating fluidized bed for continuous protein recovery, **199**, 2010, p. 32.
23. NGIAN, K. F., MARTIN, W. R., Bed expansion characteristics of liquid fluidized particles with attached microbial growth, *Biotechnol and Bioeng*, **22**, 1980, p. 1843.
24. WANG, D., MCLAUGHLIN, E., PFEFFER, R., LIN, Y. S., Aqueous phase adsorption of toluene in a packed and fluidized bed of hydrophobic aerogels, *Chemical Engineering*, **168**, 2011, p. 1201.
25. SULAYMON, A. H., MOHAMMED, T. H., JAWAD, A. H., Hydrodynamic Characteristics of Three-phase Non-Newtonian Liquid-Gas-Solid Fluidized Beds, *Emirates Journal for Engineering Research*, **15**, No. 1, 2010, pp. 41.
26. LEE, C. I., YANG, W. F., HSIEH, C. I., Removal of Cu(II) from aqueous solution in a fluidized-bed reactor, *Chemosphere*, **57**, 2004, p. 1173.
27. SULAYMON, A. H., MOHAMMED, A. A., AL-MUSAWI, T. J., "Comparative Study of Removal of Cadmium (II) and Chromium (III) Ions from Aqueous Solution Using Low-Cost Biosorbent", *Int. J. Chem. React. Eng.*, **12**, 2014, p. 1.

Manuscript received: 22.12.2018